

# Moth-Inspired Chemical Plume Tracing by Integration of Fuzzy Following-Obstacle Behavior

Wei Li and Jianwei Zhang

**Abstract**—This paper presents a strategy for chemical plume tracing (CPT) with *soft* obstacle avoidance, such as kelp forests or seaweed in near-shore, oceanic environments. The basic idea is to integrate a low-level fuzzy following obstacle behavior into a subsumption architecture for moth-inspired plume tracing. By on-line generation of dynamic reference targets (DRTs) on a course of the most recent CPT activity, an autonomous underwater vehicle (AUV) can quickly and correctly resume CPT maneuvering after passing obstacles. Simulation studies of CPT with obstacle avoidance are performed using a simulated plume with significant meander and filament intermittency in an environment with length scales of 100 m.

## I. INTRODUCTION

AQUATIC chemical plume tracking robots have been the subject of research over the last 10 years [1]. Fluid flow, featured by turbulence, tide, and even wave, significantly challenges chemical plume tracing in near-shore ocean environments. Factors that complicate CPT include the unknown chemical source concentration, the unknown advection distance of any detected chemical, and significant spatial and temporal flow variations. In order to develop an AUV-based CPT tracer for natural fluid environment application, DARPA/ONR sponsored an interdisciplinary team to investigate biologically inspired CPT strategies under the CPT program [2]-[8]. Li et al. [8] developed, optimized, and evaluated the moth-inspired *passive* and *active* plume tracing strategies, based on a single chemical sensor. The moth-inspired CPT strategies allow a single AUV to trace a chemical plume with significant meander from a potentially long distance to its initial odor source. Both the *passive* and *active* strategies were implemented on a REMUS vehicle for three in-water test runs conducted in November 2002 and April 2003 at San Clemente Island, California, and in June 2003 in Duck, North Carolina [9], [10]. The successful in-water tests demonstrated that the strategies for the tracking of chemical plumes are effective and robust to the near-shore ocean condition, as shown in Fig. 1. The accomplishment of tracing chemical plumes in a

Manuscript received December 18, 2007. This work was supported in part by the U.S. Office of Naval Research Grant ONR N00014-98-1-0820 under the ONR/DARPA Chemical Plume Tracing Program, the RCU grant at CSUB, and BMBF IVUS project.

W. Li is with the Department of Computer Science, California State University, Bakersfield, CA 93311 USA (wli@cs.csusbak.edu).

J. W. Zhang is with Institute TAMS (Technical Aspects of Multimodal Systems), Department of Informatics, University of Hamburg Vogt-Koelln-Strasse 30, D-22527 Hamburg, Germany (zhang@informatik.uni-hamburg.de).

natural environment represents a significant step toward real applications. However, CPT strategies must address obstacle avoidance issue if an AUV-based plume tracer operates in near-shore, oceanic environments. Especially, the development of CPT strategies with avoiding *soft* obstacles in near-shore ocean environments, such as kelp forests or seaweed, presents an emerging issue [11]. Some test runs conducted at SCI in August 2002 failed, as chemical filaments that were transported in turbulent fluid flow through gaps in kelp forests caused the AUV to be stuck. CPT with *soft* obstacle avoidance challenges obstacle avoidance algorithms as well as *soft* obstacle detection sensors for near-shore ocean application. CPT with obstacle avoidance is different from traditional robot path planning in the situations where a target might be specified in advance since there is no information about chemical plume and its source available prior to missions.

In an indoor environment or a small operation area, an exhaustive search approach is acceptable to scan obstacles and search for chemicals “point-by-point”. However, this approach is not practical for natural environments, since it is very time-consuming to search for plumes in a large-scale operation area, e.g., the operation area specified by 367×1094 m (greater than 60 football fields) for the in-water tests of June 2003 [10]. In the near-shore ocean environments, fluid flow magnitude and orientation change significantly, for example, fluid flow changed by almost 180° in the period from MSN009 to MSN010r1 of the SCI tests in November 2002. The significant fluid flow variation

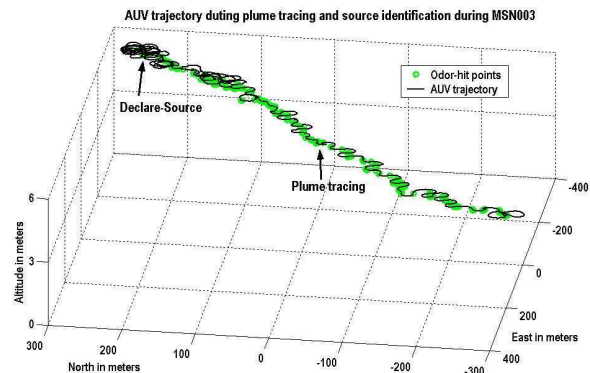


Fig. 1. An *active* moth-inspired plume tracing test conducted in near shore ocean conditions, in June 2003 in Duck, North Carolina. The Euclidian distance of plume tracing over 975 meters with source identification accuracy of approximately 13 meters

causes plumes' distributions and *soft* obstacles' locations to be changed, so an approach, which is able to dynamically search for plumes and avoid obstacles the relevant range must be more efficient than the exhaustive approach. Also, the approach has to deal with fluid flow uncertainty.

This paper presents a new strategy for CPT with obstacle avoidance by integrating a low-level fuzzy following-obstacle behavior [12] into the subsumption architecture for moth-inspired CPT. This strategy allows the AUV to quickly and correctly resume CPT maneuvering after passing around obstacles by on-line generation of dynamic reference targets (DRTs) [13] on the course of the most recent CPT activity. Simulation studies of CPT with *soft* obstacles are performed using a simulated plume with significant meander and filament intermittency in an operation area with length scales of 100 m [14].

## II. INTEGRATION OF FUZZY NAVIGATION BEHAVIORS INTO CPT ARCHITECTURE

### A. Subsumption Architecture and CPT Behaviors

Fig. 2 shows an extended version of the subsumption architecture which was implemented on the REMUS for the three field tests [9]. Before we discuss the integration of the fuzzy following-obstacle behavior into this architecture for moth-inspired CPT, we briefly review the behaviors of Find-Plume, Maintain-Plume, and Reacquire-Plume in the architecture as follows:

The heading and velocity commands  $(\theta, v)$  for Find-Plume are given

$$\theta = w_d(t, x_c, y_c) + \text{sign}(\eta)\Delta\theta(t) \quad (1)$$

$$v = v_c$$

$$\eta = 0.5(Y_{\min} + Y_{\max}) - y_c \quad (2)$$

$$\Delta\theta(t) = \begin{cases} \Delta\theta_{\text{up}} & t \in T_{\text{up}} \\ \Delta\theta_{\text{down}} & t \in T_{\text{down}} \end{cases} \quad (3)$$

$$\text{sign}(\eta) = \begin{cases} 1 & \eta \geq 0 \\ -1 & \eta < 0 \end{cases} \quad (4)$$

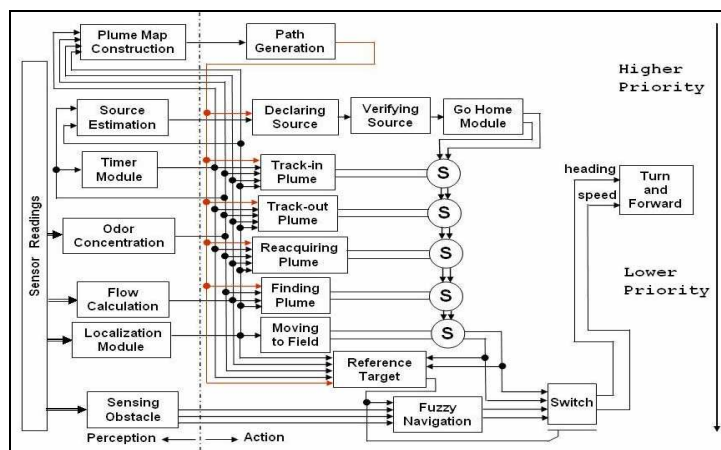


Fig. 2. Subsumption architecture for CPT with fuzzy obstacle avoidance

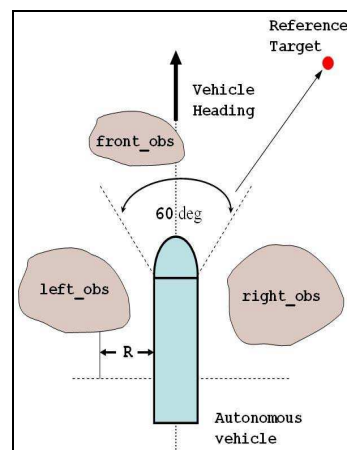


Fig. 3. Sensing obstacles for autonomous vehicle

where  $w_d(t, x_c, y_c)$  is a flow direction function of the time  $t$  and the vehicle location  $(x_c, y_c)$ ,  $\Delta\theta(t)$  is an offset angle used for up-flow or down-flow search,  $[X_{\min}, X_{\max}] \times [Y_{\min}, Y_{\max}]$  specifies an operation area, and  $T_{\text{up}}$  and  $T_{\text{down}}$  are the durations for up-flow and down-flow search.

Maintain-Plume uses two activities: Track-In and Track-Out. Their commands  $(\theta, v)$  are defined

$$\begin{aligned} \theta &= w_d(t, x_c, y_c) + 180^\circ + \Delta\theta(t)_{\text{Track-In}} \\ v &= v_c \end{aligned} \quad (5)$$

$$t \in T_{\text{above}}$$

$$\begin{aligned} \theta &= w_d(t, x_c, y_c) + 180^\circ + \Delta\theta(t)_{\text{Track-Out}} \\ v &= v_c \end{aligned} \quad (6)$$

$$t \in T_{\text{below}}$$

where  $\Delta\theta(t)_{\text{Track-In}}$  and  $\Delta\theta(t)_{\text{Track-Out}}$  are the offset angles for Track-In and Track-Out,  $T_{\text{above}}$  and  $T_{\text{below}}$  are the durations for Track-In and Track-Out activities. The *passive* and *active* strategies were defined through the selection of  $\Delta\theta(t)_{\text{Track-In}}$  and  $\Delta\theta(t)_{\text{Track-Out}}$  [8].

The commands  $(\theta, v)$  for Reacquire-Plume are defined

$$\begin{aligned} \theta &= \text{actan } 2(y_i - y_c, x_i - x_c) \\ v &= v_c \end{aligned} \quad (7)$$

where  $(x_c, y_c)$  is the current vehicle location, and  $(x_i, y_i)$  is a subgoal located on *Cloverleaf*. The cloverleaf center is  $(x_{\text{last}}, y_{\text{last}})$ , where the plume is most recently detected, and the leaf length is defined by  $d_{\text{leaf}}$ . The detail discussions on Find-Plume, Maintain-Plume, Reacquire-Plume, and Declare-Source were addressed in [9]. An inhibition mechanism arbitrates the outputs from Declare-Source to Move-To-Field.

### B. Distance Sensor Model

For CPT missions in the real world, the AUV should be equipped with "distance sensors" to detect obstacles on-line. A module, Sensing-Obstacle, in the layer of Fuzzy-

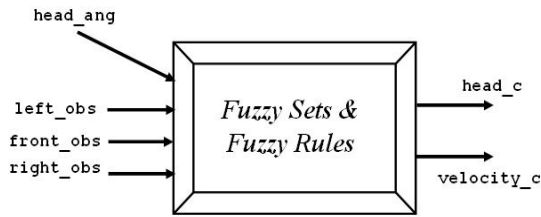


Fig. 4. Fuzzy Navigation Module

Navigation divides the distance sensors into three groups [12]. The front sensor group scans the heading area from  $-30^\circ$  to  $+30^\circ$  relative to vehicle heading direction, the left sensor group scans the left area, and the right sensor group scans the right area, as shown in Fig. 3. If the obstacles are located within the detectable distance,  $R$ , the distances between the obstacles and the vehicle in three directions are calculated by

$$\begin{aligned} \text{left\_obs} &= \min\{ds_i\} & i &= 1, 2, \dots, N_{\text{left}} \\ \text{front\_obs} &= \min\{ds_j\} & j &= 1, 2, \dots, N_{\text{front}} \\ \text{right\_obs} &= \min\{ds_k\} & k &= 1, 2, \dots, N_{\text{right}} \end{aligned} \quad (8)$$

where  $N_{\text{left}}$ ,  $N_{\text{front}}$ , and  $N_{\text{right}}$  are the numbers of scanned points on the left, front, and right directions to the vehicle, and  $ds_i$ ,  $ds_j$ , and  $ds_k$  are the detected distances from the scanned areas in the three directions.

### C. Fuzzy Behaviors

In order to navigate an autonomous system in uncertain environments, a fuzzy-logic-based behavior strategy encapsulates the behaviors: Avoid-Obstacle, Steer-Target, and Follow-Edge [12]. These behaviors are independently formulated using fuzzy sets and fuzzy rules, and their potential conflicts are coordinated through a fuzzy reasoning

TABLE I  
PARAMETERS OF INPUTS

left_obs / right_obs	(near) 5m	(med) 10m	(far) 15m
front_obs	(near) 10m	(med) 15m	(far) 20m
head_ang	(neg) $-50^\circ$	(Z) $0^\circ$	(pos) $50^\circ$

PARAMETERS OF OUTPUTS

velocity_c	(slow) 0.25m	(med) 1.2m	(fast) 2m
head_c	(neg) $-10^\circ$	(Z) $0^\circ$	(pos) $10^\circ$

mechanism. The architecture for CPT in Fig. 2 subsumes the fuzzy-logic-based strategy as the Fuzzy-Navigation module. The inputs to Fuzzy-Navigation are the detected distances between the vehicle and obstacles from three directions  $\{\text{left\_obs}, \text{front\_obs}, \text{right\_obs}\}$ , and a direction difference between a vehicle heading and a target,  $\text{head\_ang}$ . In this application, the target is specified by a DRT. The outputs from Fuzzy-Navigation are the commands for vehicle velocity and heading,  $\text{velocity\_c}$  and  $\text{head\_c}$ , as shown in Fig. 4. The membership functions defined in Fig. 5 fuzzify the inputs and outputs. Their parameters are specified in TABLE I.

The study [12] shows that Follow-Edge behavior plays an important role in driving a robot to escape from a U-shape obstacle, when the robot operates in an unknown environment. For CPT missions, the AUV needs this behavior to pass around obstacles by following their bounds. To realize this behavior, the rules from  $\{\text{Rule}^{(i)}\}$  are adopted:

- Rule<sup>(1)</sup> 1: **If** (left\_obs is far and front\_obs is far and right\_obs is near and head\_ang is neg) **Then** (head\_c is Z and velocity\_c is slow).
- Rule<sup>(1)</sup> 2: **If** (left\_obs is near and front\_obs is far

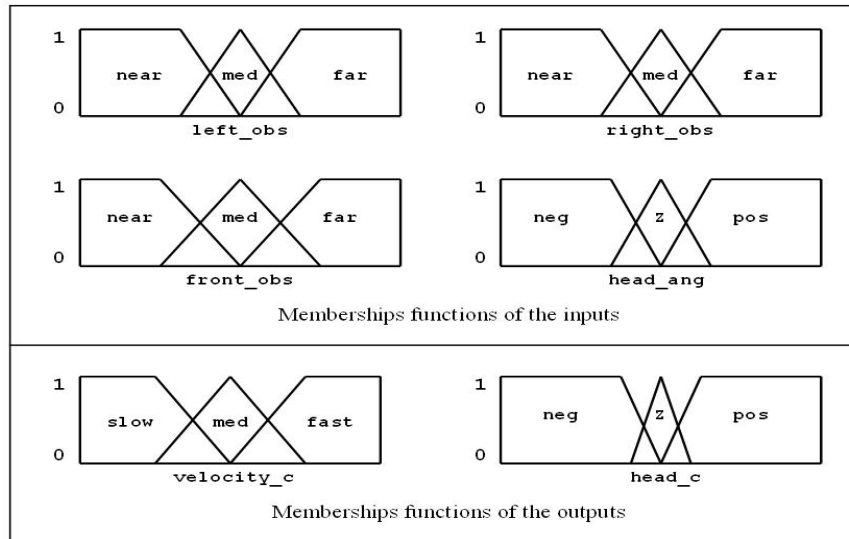


Fig. 5. Membership functions regarding inputs and outputs

- and right\_obs is far and head\_ang is pos)  
**Then** (head\_c is Z and velocity\_c is slow).
- Rule<sup>(f)</sup> 3: **If** (left\_obs is far and front\_obs is near  
and right\_obs is near and head\_ang is neg)  
**Then** (head\_c is pos and velocity\_c is slow).
- Rule<sup>(f)</sup> 4: **If** (left\_obs is near and front\_obs is near  
and right\_obs is far and head\_ang is pos)  
**Then** (head\_c is neg and velocity\_c is slow).

The Avoid-Obstacle and Steer-Target fuzzy behaviors in Fuzzy-Navigation make smooth transits in situations where detected obstacles are close to the AUV or the obstacles have been passed. To realize the Avoid-Obstacle behavior, the rules from {Rule<sup>(a)</sup> *i*} are given:

- Rule<sup>(a)</sup> 1: **If** (left\_obs is med and front\_obs is near  
and right\_obs is near and head\_ang is any)  
**Then** (head\_c is neg and velocity\_c is slow).
- Rule<sup>(a)</sup> 2: **If** (left\_obs is near and front\_obs is near  
and right\_obs is med and head\_ang is any)  
**Then** (head\_c is pos and velocity\_c is slow).
- Rule<sup>(a)</sup> 3: **If** (left\_obs is near and front\_obs is med  
and right\_obs is near and head\_ang is any)  
**Then** (head\_c is Z and velocity\_c is med).

To realize the Steer-Target behavior, the rules from {Rule<sup>(s)</sup> *i*} are adopted:

- Rule<sup>(s)</sup> 1: **If** (left\_obs is far and front\_obs is far  
and right\_obs is far and head\_ang is Z)  
**Then** (head\_c is Z and velocity\_c is fast).
- Rule<sup>(s)</sup> 2: **If** (left\_obs is far and front\_obs is far  
and right\_obs is far and head\_ang is neg)  
**Then** (head\_c is neg and vel\_c is fast).
- Rule<sup>(s)</sup> 3: **If** (left\_obs is far and front\_obs is far  
and right\_obs is far and head\_ang is pos)  
**Then** (head\_c is pos and velocity\_c is fast).

The work [12] in detail discussed how a fuzzy reasoning mechanism works to fuse the three behaviors.

#### D. Dynamic Reference Target

Specifying proper targets for Fuzzy-Navigation allows the AUV to effectively pass around obstacles during CPT missions, even though in complicated environments. If a set of random targets are specified for Fuzzy-Navigation, the

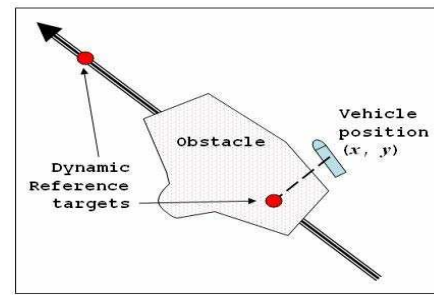


Fig. 6. DRTs and vehicle position projection on a virtual path

AUV exhibits a Wander behavior to randomly search for chemicals with obstacle avoidance, but the random-search strategy would be impractical for CPT in an operation area with a large scale. The targets for Fuzzy-Navigation must be determined during CPT missions as global information on obstacles and plumes is not available. The work [13] utilized dynamic reference targets (DRTs) to improve navigation performance. We use this idea to generate on-line DRTs for Fuzzy-Navigation by considering two issues: first, the DRT must be “behind” an obstacle since the AUV needs to pass around the obstacle, and second, the DRT should be located on the course of the most recent CPT activity as the AUV needs to correctly resume the CPT mission after passing around the obstacle. In order to generate such DRTs, we design a virtual path based on the most recent CPT mission course

$$y_{\text{path}} = \text{actan}(\theta_0) (x_{\text{path}} - x_0) + y_0, \quad (9)$$

where  $(x_0, y_0)$  is the vehicle position at  $t_0$  where the obstacle is detected the first time, and  $\theta_0$  is the vehicle orientation at  $(x_0, y_0)$ . For CPT with obstacle avoidance, a Reference-Target module generates a DRT,  $(x_g, y_g)$ , on the virtual path, to attract the vehicle toward it. The DRT,  $(x_g, y_g)$ , is ahead the current vehicle location  $(x, y)$  in the direction of  $\theta_0$ , as shown in Fig. 6. The DRT triggers concurrently the three groups of fuzzy rules in Fuzzy-Navigation. Each of them yields its own command  $(\theta, v)$  for the AUV. The fuzzy mechanism fuses the three outputs according to their weights to produce the final output. At the same time, the “Switch” module in the architecture switches its outputs from the Plume-Find, Maintain-Plume, or Reacquire-Plume behavior to the fuzzy navigation behaviors. Once the AUV reaches  $(x_g, y_g)$  in the direction of  $\theta_0$ , i.e., the  $(x, y)$  projection on the virtual path reaches  $(x_g, y_g)$ , during the AUV maneuvering, Reference-Target updates  $(x_g, y_g)$  by increasing a distance of 15m in the direction of  $\theta_0$ . Note that reaching  $(x_g, y_g)$  means

TABLE II  
PARAMETERS FOR CPT BEHAVIORS

Find-Plume	Maintain-Plume	Reacquire-Plume	Declare-Source
Up-flow search offset: $\Delta\theta_{\text{up}} = \pm 125$ deg	Waiting time: $\lambda = 8.5$ s	Diameter of the cloverleaf $d_{\text{leaf}} = 15$ m	Sorted point number $M = 6$
Down-flow search offset: $\Delta\theta_{\text{down}} = \pm 60$ deg	$\Delta\theta(t)_{\text{Track-In}} = 0$ deg $\Delta\theta(t)_{\text{Track-Out}} = \pm 10$ deg Threshold = 0.20	Repetition number: $N_{\text{re}} = 3$	Source estimation criterion $\epsilon = 5$ m

that the AUV passes around the obstacle. Then it resumes the most recent CPT activity and deactivates the Reference-Target module.

### III. SIMULATION STUDIES

We perform simulation test runs to evaluate the performance of the proposed CPT architecture using a simulated plume. An operation area is specified by  $[0, 100] \times [-50, 50]$  in meter, as shown in Fig. 6. Some black objects represent *Soft* obstacles in the operation area. The filament release rate is 5 filaments/s, the simulation time step is 0.01 s, and the mean fluid velocity 1 m/s. During the simulation studies, the measured fluid flow is corrupted by additive noise that is white normal random process. The field of small arrows on the figure indicates the direction of the local fluid flow vector at the tail of each arrow. The fluid flow vector varies spatially, and the correlation of the fluid flow direction and plume axis direction decreases with the distance from the source. The heading command for the vehicle orientation,  $\theta$ , is limited to  $[-180^\circ, 180^\circ]$ , and the velocity command for the vehicle speed is set between 1.0m and 1.5m. The parameters of the CPT behaviors are listed in Table II.

A graphic “snapshot” in Fig. 7(a) illustrates a test run with obstacle avoidance while Find-Plume is active. The AUV starts its CPT mission at a home location, and activates Find-Plume to search for the plume in the entire operation area. Reference-Target uses a virtual path to determine a DRT on the course of Plume-Find when the AUV detects the obstacle. The following scenario illustrates that Fuzzy-Navigation works correctly. When the AUV approaches the obstacle, Avoid-Obstacle dominates the outputs from Fuzzy-Navigation, which drive the AUV to make a turn to avoid the obstacle. When the AUV heads in an obstacle-free direction, the DRT weights the outputs of Follow-Edge from Fuzzy-Navigation to control the AUV to follow the obstacle bounds. The AUV goes around the obstacle and moves toward the DRT. When the AUV reaches the DRT, it resumes the most recent CPT activity, Find-Plume. The

sensed concentration activates Maintain-Plume to navigate the AUV toward the plume source in up-flow direction. During this activity, the AUV detects another obstacle. Reference-Target determines a new DRT on the course of the plume-tracing activity for Fuzzy-Navigation.

A “snapshot” in Fig. 7(b) illustrates another test run of *soft* obstacle avoidance while Maintain-Plume is active. Assuming that the objects in the operation area are kelp or seaweed, fluid-advected filaments are transported through gaps of those *soft* obstacles. The subsumption architecture switches Find-Plume to Maintain-Plume, when the AUV senses the plume concentration. Maintain-Plume uses both the Track-In and Track-Out activities to maintain contact with the plume and to move up-flow toward the odor source. When the AUV is approaching the *soft* obstacle located on the course of the plume-tracing activity, Avoid-Obstacle drives the AUV away from the course to avoid the obstacle. At the same time, Reference-Target uses a virtual path to generate a DRT on the course to attract the AUV, and then Follow-Edge navigates the AUV to follow the bounds of the obstacle. It moves toward the DRT after passing the obstacle. The AUV detects a new obstacle when it gets close the DRT. A new DRT on the virtual path is created to navigate the AUV to follow the bounds of the new obstacle. The AUV resumes the plume-tracing activity successfully, when it reaches the new DRT. Should the AUV be unable to detect the plume near the location of the new DRT, it would activate the Reacquire-Plume behavior. The Reacquire-Plume behavior would continue for several seconds to reacquire the plume around the DRT. The two test runs are conducted in the fluid-advected environment with the same obstacle distributions, but the trajectories recorded during the test runs are quite different due to fluid flow with location and time variations, and significant plume meander, as shown in Fig. 7.

### IV. DISCUSSIONS AND CONCLUSIONS

The tracking of fluid-advected plumes in the near-shore ocean environments requires an olfaction-based navigation algorithm to integrate measured fluid flow information.

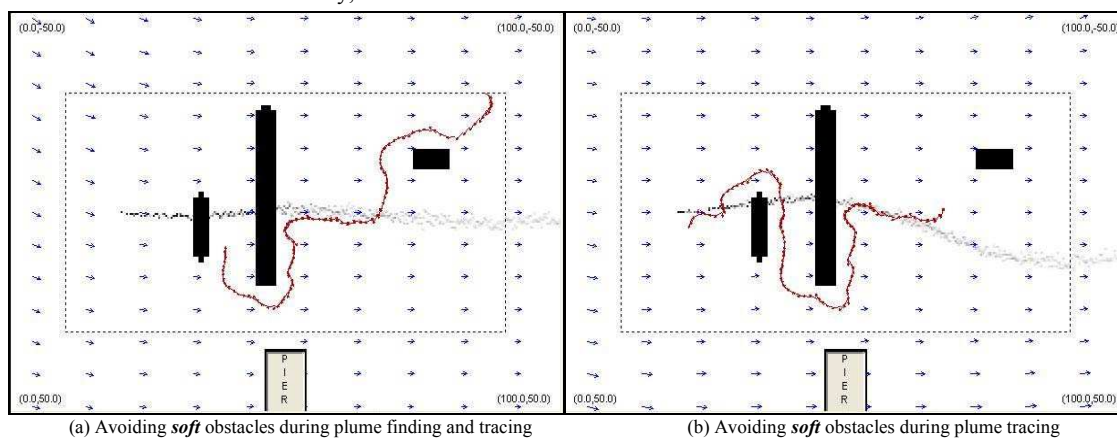


Fig. 7. A plume with a significant meander is transported through the gaps in the *soft* obstacles



Some researchers used laboratory robots to test their CPT strategies and reported plume-tracing distances within few meters. However, CPT strategies developed and tested in a laboratory-structured environment may not be directly applicable for natural environments since fluid or air flow generated in the laboratory-structured condition may not effectively represent natural fluid flow in near-shore, oceanic conditions featured by turbulence, tides, and even waves. Development and evaluation of CPT strategies using a simulated fluid environment are an effective and efficient means. Considering natural fluid conditions, our simulated fluid flow environment addresses the three factors that challenge the tracking of chemical plumes: 1) significant intermittency of filaments; 2) significant plume meander due to a long distance transportation of filaments; 3) significant variation of flow magnitude and orientation plus random noise. As a result of our simulation studies, in an operation area with scales of few meters, many “zigzag path” resembled tracing strategies may navigate a searcher to reach the plume source, even by the very simple rules: if the robot detects chemicals, it moves up-flow; if the robot loses contact with chemicals, the robot moves cross-flow. However, such an implementation might not work for the natural environments with the large scales, as the correlation of the fluid flow direction and plume axis direction decreases with the distance from the source.

Chemical plume tracing with *soft* obstacle avoidance is an emerging issue in designing CPT strategies. The effects of hard obstacles on CPT are distinct from those of soft obstacles. Zarzhitsky et al. [15] presented a fluid dynamics model for chemical plume tracing with hard obstacle avoidance. In this model, tangential flow around the obstacles carries chemical filaments passing around the obstacles when fluid flow hits hard obstacles. Consequently, a path to trace the plume following up-tangential-flow direction may guide the AUV to pass around the hard obstacles in operation areas. However, this model is not suitable for CPT with *soft* obstacle avoidance, since fluid flow carries some chemical filaments through *soft* obstacles, such as kelp forests in ocean environments, which may cause the AUV to become stuck during plume-tracing in the up-flow direction.

Fuzzy-logic-based behavior strategies are widely accepted for robot navigation in uncertain environments, but rarely applied to CPT. Individual experiments on CPT and Fuzzy-Navigation behaviors via robot systems were separately reported in the literatures. CPT test runs with obstacle avoidance in natural environments need to develop sensors for detecting obstacles underwater, including both *soft* obstacles and hard obstacles. Distance sensors, e.g., sonar sensors, are able to detect hard obstacles, but might not work well for *soft* obstacles. Sensing *soft* obstacles presents a significant challenge to the current marine sensors. A visual sensor would be possible to detect *soft* obstacles. However, processing images taken in near-shore, ocean conditions is a very challenging task, since the propagation of light underwater is complicated by three phenomena which affect

both the illuminant and the light rays reflected from the object to the sensor: scattering, refraction, and absorption [16]. These facts cause interpretation of color images of real scenes taken in near shore ocean environments usually incomplete and ambiguous [17], and consequently it is very hard to reliably determine which color belongs to and which does not belong to obstacles. Furthermore, the AUV operates in deep water from few meters to over twenty meters to search and trace chemicals. Detecting obstacles using a visual sensor under conditions requires the AUV to use a very powerful lighting system to illuminate dark environments during CPT missions. However, a small and light underwater vehicle has very limited power supply.

#### REFERENCES

- [1] T. R. Consi, F. Grasso, D. Mountain, and J. Atema, “Explorations of turbulent odor plumes with an autonomous underwater robot,” *Biological Bull.*, vol. 189: pp. 23 1-232, 1995.
- [2] E. A. Cowen and K. B. Ward, “Chemical Plume Tracing,” *Environmental Fluid Mechanics*, vol. 2, no. 1-2, pp. 1-7, 2002
- [3] F. W. Grasso, T. R. Consi, D. C. Mountain, and J. Atema, “Biomimetic robot lobster performs chemo-orientation in turbulence using a pair of spatially separated sensors: Progress and challenges,” *Robotics and Autonomous Systems*, vol.30, pp.115-131, 2000.
- [4] F. W. Grasso and J. Atema, “Integration of flow and chemical sensing for guidance of autonomous marine robots in turbulent flows,” *Journal of Environmental Fluid Mechanics*, vol.1, pp.1-20, 2002.
- [5] Q. Liao and E. A. Cowen, “The information content of a scalar plume – A plume tracing perspective,” *Environmental Fluid Mechanics*, vol. 2, no. 1-2, pp. 9-34, 2002.
- [6] M. J. Weissburg *et al.*, “A multidisciplinary study of spatial and temporal scales containing information in turbulent chemical plume tracking,” *Environmental Fluid Mechanics*, vol. 2, no. 1-2, pp. 65-94, 2002.
- [7] A. T. Hayes, A. Martinoli, and R. M. Goodman, “Distributed chemical source localization,” *IEEE Sensors Journal*, vol. 2, pp. 260-271, 2002.
- [8] W. Li, J. A. Farrell, and R. T. Cardé, “Tracking of fluid-advected chemical plumes: Strategies inspired by insect orientation to pheromone,” *Adaptive Behavior*, vol.9, pp.143-170, 2001.
- [9] W. Li, J. A. Farrell, S. Pang, and R. M. Arrieta, “Moth-inspired chemical plume tracing on an autonomous underwater vehicle”, *IEEE Transactions on Robotics*, vol.22, no.2, pp.292-307, 2006.
- [10] J. A. Farrell, S. Pang, and W. Li, “Chemical plume tracing via an autonomous underwater vehicle,” *IEEE Journal of Ocean Engineering*, vol.30, pp.428-442, 2005.
- [11] W. Li and D. Carter, “Subsumption architecture for fluid-advected chemical plume tracing with soft obstacle avoidance,” in *Proc. of Ocean Marine Technology and Ocean Science Conference*, 2006.
- [12] W. Li, “Fuzzy-logic-based reactive behavior control of an autonomous mobile system in unknown environments,” *Engineering Application of Artificial Intelligence*, vol.7, no.5, pp. 521-531, 1994.
- [13] W. Li, C. Y. Ma, and F. M. Wahl, “A neuro-fuzzy system architecture for behavior-based control of a mobile robot in unknown environments,” *Fuzzy Sets and Systems*, vol. 87, pp. 133-140, 1997.
- [14] J. A. Farrell, J. Murlis, X. Long, W. Li, and R. Carde: “Filament-Based Atmospheric Dispersion Model to Achieve Short Time-Scale Structure of Chemical Plumes,” *Environmental Fluid Mechanics*, vol.2, pp.143-169, 2002.
- [15] D. Zarzhitsky, D. F. Spears, and W. F. Spears, “Distributed robotics approach to chemical plume tracing,” in *Proc. of Int. Conf. on Intelligent Robots and Systems*, 2005
- [16] T. T. Team, “The physics of diving: Light and vision,” <http://library.thinkquest.org/28170/35.html>.
- [17] J. S. Jaffe, et al., “Underwater optical imaging: status and prospects”, *Oceanography*, vol. 14, pp. 64-75, 2002.